

Experimental Characterization of Thermal Creak Response of Deployable Space Structures

Michel D. Ingham,* Yool A. Kim,[†] Edward F. Crawley,[‡] Hugh L. McManus,[§] and David W. Miller[¶]
Massachusetts Institute of Technology, Cambridge, Massachusetts 02139

The phenomenon of thermal creak in deployable space structures is investigated. Thermal creak is a disturbance that occurs when thermally induced stress in a statically indeterminate structure is suddenly released via a slip internal to a joint or other frictional mechanism. A representative deployable truss is suspended in a thermal chamber, where its temperature is cycled, in order to determine whether thermal creak occurs in such a structure. High-bandwidth accelerometers distributed across the truss are used as the primary sensors for detecting structural events. Thermal creaks are found to occur during the thermal transients before steady state is achieved throughout the truss. The truss response to the impulsive and broadband disturbances is characterized in both the time and frequency domains. The transient response exhibits telltale signs of structural behavior, including multimode or dominant-mode excitation, and reasonable modal damping in the time decay. An analytical model of the thermal creak mechanism is presented that qualitatively captures the structural behavior.

Nomenclature

F_k	= kinetic friction force, N
F_s	= static friction force, N
f_k	= ratio between kinetic and static friction
k_i	= stiffness of component i , N/m
m_i	= modal mass of component i , kg
α_i	= coefficient of thermal expansion of component i , $(^\circ\text{C})^{-1}$
ΔT_i	= change in temperature of component i , $^\circ\text{C}$
κ	= stiffness ratio between components 1 and 2
μ	= mass ratio between components 1 and 2

Introduction

BECAUSE of stringent size limitations imposed by launch rocket shrouds or space shuttle payload bays, most spacecraft require deployment mechanisms for their extended appendages. For instance, solar arrays are typically unfolded once a satellite is released from the shroud or payload bay. In particular, future precision space structures, such as the 10-m baseline interferometer planned for the Space Interferometry Mission,¹ will require on-orbit deployment capability. These precision structures will have very stringent dimensional stability requirements. Identifying and understanding all on-orbit disturbances are therefore critical steps in the design process for such spacecraft.

Statically indeterminate deployable structures are particularly susceptible to a broadband thermally induced disturbance known as thermal creak. As the thermal load on a space structure changes, perhaps caused by the change in radiation environment as the spacecraft passes in or out of the Earth's shadow, the structure tries to contract or expand as dictated by the coefficients of thermal expansion (CTE) of its components (see model in Fig. 1). Because of a mismatch in CTE between components made of different mate-

rials (α_1, α_2), free thermal expansion is not allowed to occur, and stresses are created in the structure. This stress buildup can also occur because of nonuniform heating or cooling across a structure ($\Delta T_1, \Delta T_2$), even one composed of a single material, perhaps as a result of partial shadowing. If there are frictional interfaces in the load path between stressed elements, a level of internal load can be attained such that the static friction force F_s is exceeded. The two elements then experience a sudden slip along the friction interface, which releases the built-up stress, until the slip is halted because of one of two reasons: either enough stress is relieved such that the internal load falls below the level of the dynamic friction F_k , or the end of the frictional deadband is reached (i.e., the fixed boundary of the interface is contacted). This slip releases some of the thermally induced elastic energy stored in the stressed elements and translates an impulsive disturbance internal to the structure. This nonlinear phenomenon is not to be confused with the linear phenomenon of thermoelastic shock, where global response of a flexible structure occurs because of rapidly changing temperature load.^{2,3} In the book by Thornton,⁴ a thorough historical review of research in thermally induced structural vibrations is presented.

Thermal creak is a potentially serious problem, especially for deployable and flexible space structures. These structures typically have numerous potential creak elements: nonlinear joints with deadbands, tensioning cables and pulleys, and other structural elements that depend on friction. The poor understanding of this type of disturbance is exacerbated because thermal creaks have rarely, if at all, been directly observed. Their nature must generally be inferred from the spacecraft sensors and the control system response.⁴ For instance, an anomalous behavior was observed in the Hubble Space Telescope rate gyro data.⁵ Small disturbances were detected throughout the orbital day, which were attributed to thermal creak in the solar array deployment mechanism.

A simple model of thermal creak was developed⁶ to understand the mechanism and to identify the key parameters. The analytical study showed that the creak response introduces a step disturbance to the structure, hence exciting all of the structural modes. Further, these step disturbances can occur successively throughout the thermal transient, until thermal equilibrium is attained. The nondimensional key parameters that dictate the behavior are 1) the thermal strain ratio between the components, 2) the stiffness ratio between the components $\kappa = k_2/k_1$, 3) the mass ratio between the components $\mu = m_2/m_1$, and 4) the ratio between the kinetic and static friction $f_k = F_k/F_s$. Parametric studies indicated that a wide range of behavior can result and that the exact nature of the system response to thermal creak is case specific.⁷

To date, very little work has been done to characterize thermal creak disturbances. Considering their potentially serious repercussions on the success of future precision space structures, on-orbit and

Presented as Paper 99-1269 at the AIAA/ASME/ASCE/AHS/ASC 40th Structures, Structural Dynamics, and Materials Conference, St. Louis, MO, 12–15 April 1999; received 12 May 1999; revision received 11 February 2000; accepted for publication 20 February 2000. Copyright © 2000 by the American Institute of Aeronautics and Astronautics, Inc. All rights reserved.

*Graduate Research Assistant, Space Systems Laboratory, Department of Aeronautics and Astronautics. Student Member AIAA.

[†]Graduate Research Assistant, Space Systems Laboratory, Department of Aeronautics and Astronautics; currently Senior Engineer, Orbital Sciences Corp., 20301 Century Boulevard, Germantown, MD 20874. Member AIAA.

[‡]Professor and Department Head, Space Systems Laboratory, Department of Aeronautics and Astronautics. Fellow AIAA.

[§]Principal Research Scientist, Space Systems Laboratory, Department of Aeronautics and Astronautics. Associate Fellow AIAA.

[¶]Assistant Professor, Space Systems Laboratory, Department of Aeronautics and Astronautics. Member AIAA.

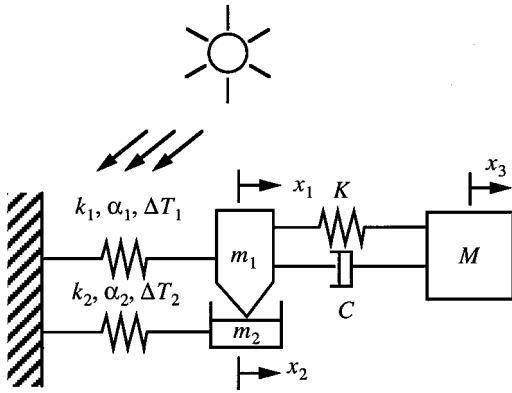


Fig. 1 Simplified structural model of a thermal creak mechanism. Stress builds in the structure as a result of CTE mismatch or nonuniform temperature load. When a level of internal load is attained such that F_s is exceeded at the interface of elements 1 and 2, the two elements experience a sudden slip, which translates an impulsive disturbance to the rest of the structure (represented as equivalent mass M , damping C , and stiffness K).

on-ground experiments must be conducted to better understand the nature of the phenomenon and the resulting system dynamics. One such on-orbit experiment, the Interferometry Program Experiment II (IPEX-II), was conducted by researchers from the Jet Propulsion Laboratory in August 1997, during the STS-85 shuttle mission.⁸ One of the main objectives of the experiment was to monitor a deployable truss structure for thermal creak-induced vibrations. The flight experiment demonstrated that thermal creak events occurred on the preloaded deployable truss and that the structural response varied from event to event. Ground-based experiments were conducted at the Massachusetts Institute of Technology in order to demonstrate thermal creak in a controlled laboratory environment and to characterize the ensuing structural response. A representative deployable truss structure was chosen as the test article for these experiments. The objective of this paper is to present the results from this series of on-ground experiments. The insights gained from this investigation will aid in developing disturbance attenuation and mitigation strategies.

Approach

To demonstrate thermal creak in a preloaded deployable truss structure, a representative truss was suspended in a thermal chamber and subjected to a temperature environment traceable to that encountered by a realistic spacecraft. Accelerometer sensors distributed across the structure were used to detect any creak events. The ensuing structural response was characterized by traditional techniques, in both the time and frequency domains.

Hardware Description

The deployable truss shown in Fig. 2 was chosen as the testbed for this investigation of the phenomenon of thermal creak. The four-bay module is composed of Lexan struts with aluminum joints and steel-wire diagonals. The test article is 81.3 cm long in its deployed state and weighs approximately 1.4 kg. Its cross section is a square, 20.3 cm on a side. The different materials composing the module have significant mismatch in their CTEs: $62.5 \times 10^{-6} \text{ }^\circ\text{C}^{-1}$ for the Lexan struts, $23.6 \times 10^{-6} \text{ }^\circ\text{C}^{-1}$ for the aluminum joints, and $14.5 \times 10^{-6} \text{ }^\circ\text{C}^{-1}$ for the steel diagonals. The design of the structure includes a number of nonlinear frictional mechanisms (examples shown in Figs. 3 and 4), which present the potential for thermal creak. A more thorough description of the truss can be found in Ref. 9. The truss was suspended from its upper four corners, using steel springs that provided a fundamental bounce mode around 2 Hz.

Thermal Source

To apply thermal load to the test article, it was suspended in a chamber where the temperature environment was controllable. Two test facilities with different heat-transfer mechanisms were used. A first series of tests was performed in a thermal chamber, which

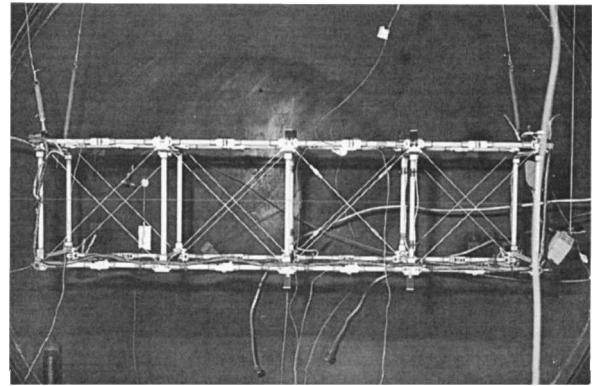


Fig. 2 Deployable truss module suspended in the thermal vacuum chamber.

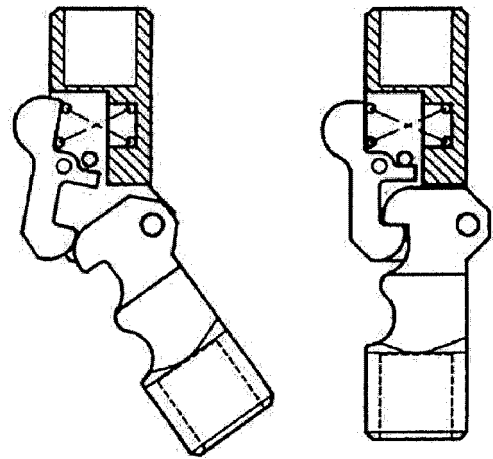


Fig. 3 Longerons knee joint and latch mechanism.

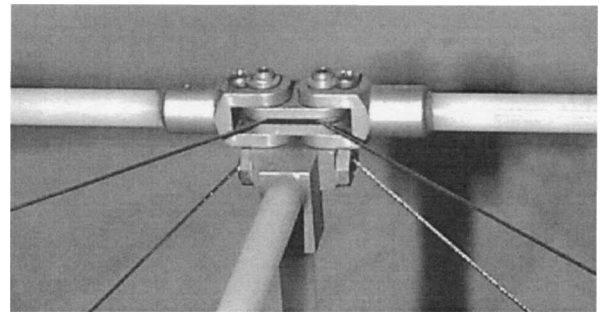


Fig. 4 Pin-clevis joints at the ends of each longeron.

used forced convection to change the temperature of the structure. The temperature inside the chamber was regulated via a controlled system, in which air was heated or cooled and circulated through the chamber with fans. The second series of tests was performed in a thermal vacuum chamber where heating and cooling of the truss was accomplished via radiation, at pressures less than 10^{-4} torr. The structure was suspended inside a cylindrical aluminum shroud lining the inside of the chamber walls. The shroud was cooled or heated by circulating liquid nitrogen or hot nitrogen gas, respectively, through tubes on its outer surface. Radiation heat flow was thus established between the structure and the black-painted inner surface of the shroud.

Sensors and Data Acquisition

Various combinations of accelerometers, strain gauges, and thermocouples were used throughout the series of tests to acquire information on the events, as well as on the temperature and stress state of the truss. Two types of accelerometers were used to measure the vibration response of the test article: accelerometers labeled

type A (with bandwidths from 0 to 500 Hz) and type C (from 5 to 8000 Hz). No correction was made to the sensitivities of either type of accelerometer to account for temperature effects, but the amount of acceleration amplitude error introduced by these effects should be less than 5% over the temperature range of interest, based on the manufacturer's specifications.

A high-bandwidth data acquisition system with triggering capability was used, which allowed accelerometer data channels to be recorded simultaneously when a user-defined threshold signal level was exceeded on one predetermined channel. An improvement to the data acquisition system was added for some of the later tests in the thermal vacuum chamber, allowing triggering to occur upon detection of an event by any of the accelerometers.

Measures Taken to Identify Thermal Creak

In an investigation of this kind, great care must be taken to ensure that vibration events caused by the phenomenon of interest—thermal creak, in this case—can be identified as such. This section highlights the recognizable characteristics of thermal creak events and briefly describes some of the different measures taken to distinguish events caused by thermally induced structural vibrations from events caused by other sources.

Although a review of the literature has turned up very few actual observations of the phenomenon, certain expected characteristics of thermal creak can be identified, through knowledge of a structure and its frictional mechanisms, combined with simple models of the disturbance, such as those developed in Ref. 6. Thermal creak only occurs once a critical level of internal stress is reached in an indeterminate structure; the creak event is therefore expected to occur during a temperature transient, after stress has built up over some time, but before steady state has been attained. Correlating the time of occurrence of an event and the temperature state of the structure at that instant should provide a first indication of the likelihood that an observed event is caused by thermal creak. Another indication is provided by the time- and frequency-domain analyses of the event signal. Because thermal creak is an impulsive (i.e., broadband) structural disturbance, the time trace and frequency spectrum should reflect the telltale signs of structural response: multimodal, lightly damped harmonic vibration.

With the expected characteristics of the phenomenon of interest identified, the next step is to identify all of the nonthermally induced disturbance sources in the tests. If these sources can be eliminated, or if the signals caused by these sources can be distinguished from those caused by thermal creak, then it ensures that the objectives of this investigation (demonstration and characterization of thermal creak) can be met. A thorough discussion of the different possible nonthermally induced disturbances is given in Ref. 10, along with the various measures taken to mitigate/identify them. In this section the two most significant sources are addressed: transmission of mechanical vibrations to the truss and electrical events.

Transmission of Mechanical Vibrations

The thermal chambers provide a significant background vibration environment caused by the various heaters, pumps and compressors they employ. During the tests, transmission of these vibrations to the truss could only occur through the suspension springs or the various sensor wires running from the truss to the chamber walls. A number of measures were in place to eliminate as much of the transmitted disturbance as possible. First of all, the transmissibility roll off of the suspension system would greatly attenuate any chamber vibration, particularly in the high-frequency range of interest. Also, care was taken to keep enough slack in the accelerometer cables and thermocouple wires leading off the structure to avoid an accidental load path. In addition to these two attenuating effects, extra precautions were put in place to identify any chamber-induced vibration, should it somehow be detectable on the truss. Accelerometers were always mounted at either end of one suspension spring (on the chamber ceiling and the truss corner fitting) to correlate any structural vibrations with chamber vibrations. In addition, for a number of the convection tests, a dummy truss bay was suspended next to the deployable truss and instrumented with accelerometers. This bay was made of Lexan struts bonded to aluminum corner nodes with no non-

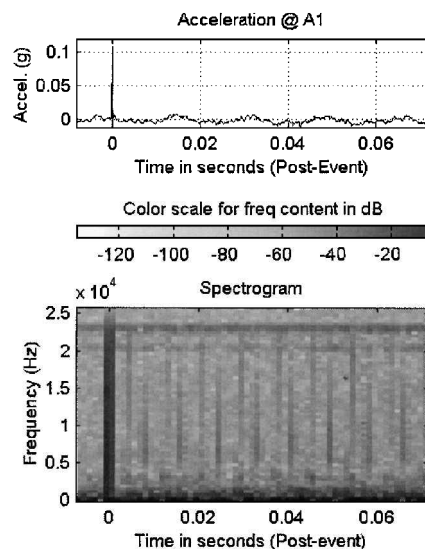


Fig. 5 Sample electrical event.

linear mechanisms. A true thermal creak would only be detected on the deployable truss and not on the nominally linear dummy structure.

Electrical Events

Another type of disturbance was the pickup of electrical signals by the sensors or their wiring. Electrical disturbances were unavoidable in an experiment of this type; the data acquisition system was susceptible to false triggering, because of electrical events, such as those associated with activation of valves or pumps from the chamber.

Although electrical disturbances could not be eliminated, they were fairly easy to identify, fortunately. Such events were evident as very sharp spikes in the data, which exhibited very little of the exponentially decaying ringing one would expect from a structural disturbance. Figure 5 shows an example of an event identified as electrical in origin, correlated with the activation of a pump from the convection chamber. One accelerometer signal is presented, with frequency content given in the form of a spectrogram plot. The spectrogram, obtained by computing Fourier transforms of a signal over short time intervals, provides estimates of the short-term, time-localized frequency content. Each vertical slice through the plot represents the spectrum computed from a time interval spanning 128 data points for frequencies ranging from 0 Hz up to half the sampling frequency. Darker shaded areas represent more significant content at a given frequency. On the time trace the event appears as a very sharp impulse; this impulse translates to a short-duration broadband frequency response visible on the spectrogram. However, no structural ringing or multimode behavior is excited, distinguishing this type of event from a thermal creak.

Experimental Results

The thermal tests yielded a number of events identified as thermal creak. In this section results are presented for two typical events, one from each of the convection and radiation tests, respectively. A summary of the findings from the full suite of tests is then presented.

Convection Test

The results from one typical convection test are presented in this section. Temperature profiles for the ambient air and the surface of the truss are shown in Fig. 6. A single thermocouple was used to monitor the surface temperature of the structure because the convection chamber provided a reasonably uniform thermal load to the test article. There was very little difference between the truss surface and ambient temperatures because of the effectiveness of the forced convection heat transfer. Grey vertical lines in the figure indicate times when events were detected and recorded. To avoid damage to the test article by exceeding design stress limits, a conservative upper limit on temperature was set. It was therefore reasoned that thermal creak would be more likely to occur during the cooling process,

when the change in stress with respect to the nominal (room temperature) stress would be greater. Throughout the tests the majority of events were detected while the truss was being cooled.

Figure 7 presents the truss response data corresponding to the event occurring approximately 157 min into the test. The figure also shows the sensor distribution across the deployable truss. Five accelerometers were used to detect thermal creaks on the deployable module (C2, C3, C4, A1, and A6, labeled so as to indicate their type). The arrows in the figure denote the direction of action for each accelerometer. Another accelerometer (C1) was placed on the chamber ceiling, at the base of one of the springs (not shown in figure). Finally, the dummy bay was instrumented with two more accelerometers, C5 and C6 (also not shown).

No sign of the event was seen in the signals from the accelerometers on the chamber ceiling and the dummy truss (C1, C5, and C6), even though evidence of an impulsive disturbance was clearly observed by all of the sensors on the deployable truss (C2, C3, C4, A1, and A6). This evidence points to a structural source for the disturbance, rather than a vibration acoustically or mechanically transmitted to the truss from the surrounding thermal chamber environment.

The general location of the disturbance source can be inferred by comparing the magnitudes and the frequency content of the response at different accelerometer channels. Based on the time traces in Fig. 7, it appears that the thermal creak occurred roughly midway along the length of the truss, in the vicinity of C3 and C4. These two traces exhibit the highest-amplitude transients (maximum amplitudes around 2 g) and are the signals most dominated by high-frequency response, as expected in proximity of the disturbance source. High-frequency content is filtered as the disturbance propagates away from the source caused by the dispersive effects of the medium and the joints.¹¹ A comparison between the start times

of the event as measured by the sensors supports the deduction that the event occurred near C3: zooming in on the traces reveals that the event began 0.7 ms later at C2 and A6 than at C3. The truss response can also be characterized in the frequency domain. Figure 8 shows the spectrograms of the accelerometer time traces from Fig. 7. Accelerometer A1 shows more high-frequency content than C2 and A6 (see Fig. 8), suggesting that the creak acted predominantly in the horizontal, transverse direction with respect to the deployable truss (in the sensing direction of A1, C3, and C4, perpendicular to the sensing directions of C2 and A6).

In Fig. 8 the C3, C4, and A1 spectrograms show that various modes between 10 and 23 kHz were excited by the creak. In general, the dark spots occur at different frequencies for different sensors, indicating that these high-frequency modes are predominantly local. In particular, the C3 trace shows strong modal response around 10.5 kHz in the initial transient. By bandpass filtering the C3 time trace, and fitting an exponentially decaying sinusoid function, a damping ratio estimate of approximately 1% is obtained for this mode, a reasonable value for structural damping (a viscous damping model is assumed). Although the poor resolution of the spectrograms makes it difficult to characterize the low-frequency content accurately, it is evident that all of the accelerometers on the deployable truss picked up significant response below 3 kHz or so.

This typical event was the first in a sequence of events picked up during the second cooling phase of the thermal test (see Fig. 6). All of these sequential events looked very much alike in terms of the shape and frequency content of the response time traces, except that the overall magnitude of response seemed to decrease with each successive event. Additionally, each pair of successive creaks exhibited the trend of increasing separation in time. This type of behavior points to the possibility of repeated creaking of one slip interface over the temperature transient, with increasing time intervals between slips as the structure approached steady-state temperature. The time elapsed between successive slips of a single interface is referred to as the creak period. Thus, even in a nominally symmetric and repeated structure, like the deployable module, some joints are more at risk than others for experiencing thermal creak, perhaps because of differences in the friction parameters at the interface or slight asymmetries in the internal stress distribution. Similar successive impulsive disturbances, exhibiting the general trends of decreasing amplitude and increasing creak period, were observed on the Hubble Space Telescope during its initial on-orbit checkout; these impulsive events, which occurred during the orbital day, were attributed to thermal creak in the solar array spreader bars.⁵

Radiation Test

This section presents results from one typical radiation test. The thermal responses of the truss structure and the radiation shroud of

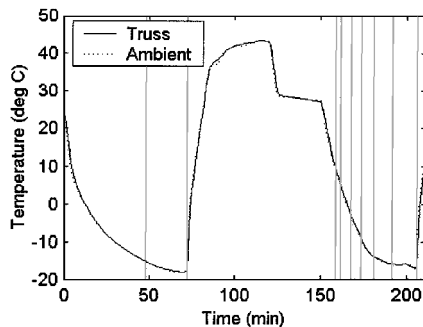


Fig. 6 Temperature histories for a typical convection test. Vertical lines indicate times where transient events occurred.

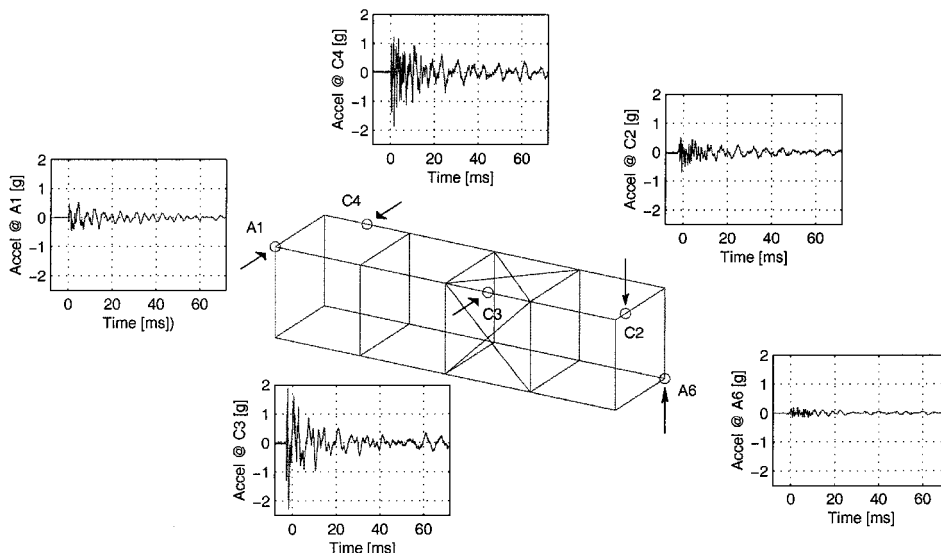


Fig. 7 Thermal creak data from a typical convection test.

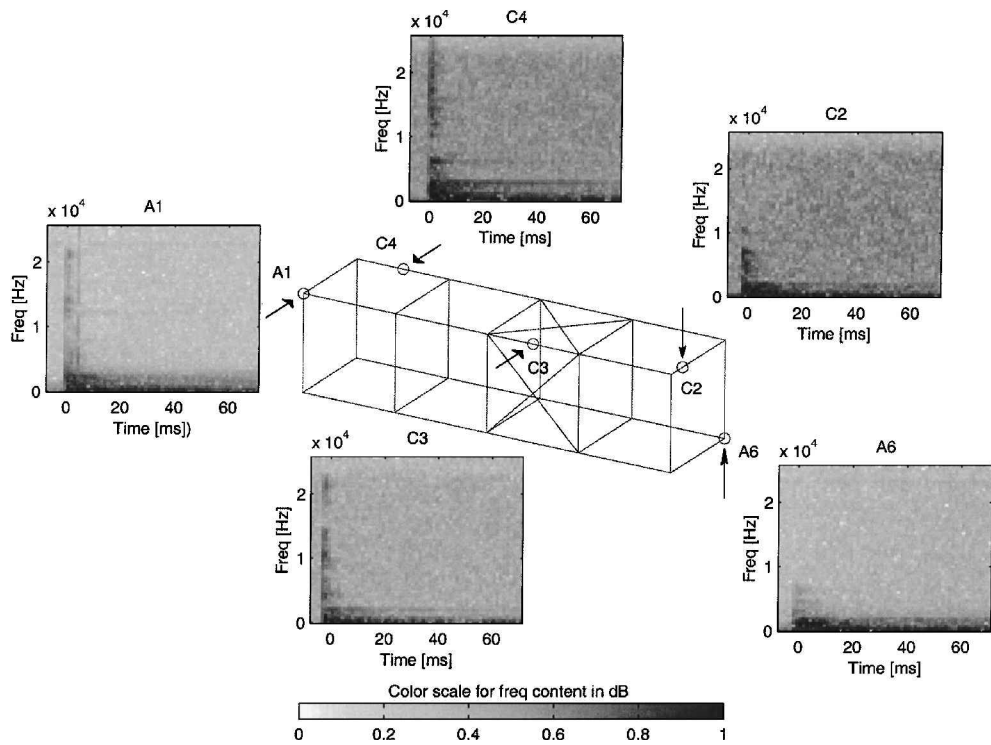


Fig. 8 Thermal creak event spectrograms from a typical convection test.

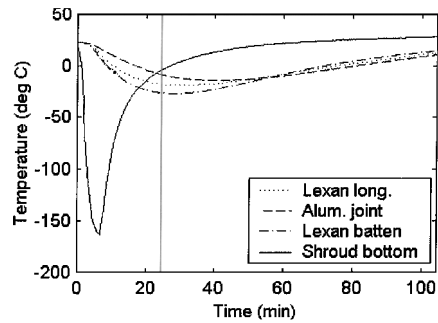


Fig. 9 Temperature histories for a typical radiation test. Vertical line indicates time where transient event occurred.

the thermal vacuum chamber are plotted in Fig. 9. Two thermocouples were bonded to one of the longerons, on a Lexan strut and an aluminum joint, respectively, whereas another thermocouple was attached to a Lexan batten member. To simulate a sudden, significant thermal transient, such as would be encountered by a spacecraft entering and exiting planetary eclipse, an impulsive thermal load was applied to the test article. The temperature distribution across the test article was noticeably more nonuniform than for the convection tests. The lowest truss temperature was measured on the Lexan batten, which dropped to just under -25°C after approximately 30 min.

During this test, one event was identified as thermal creak. It occurred approximately 23 min into the test, as indicated by the vertical grey line in Fig. 9. Figure 10 shows the dynamic response of the structure as measured from four accelerometers. The oscillatory signal evident in all four traces is actually electrical line noise at 60 Hz, which was picked up by the sensor wires. As expected for a thermal creak occurring on the test article, the trace from the accelerometer placed on the chamber shroud (C1) shows no sign of the event. Unlike the events recorded during the convection tests, only one accelerometer on the truss detected the broadband creak: the impulsive event with peak amplitude around 1 g is clearly evident in the trace from accelerometer C4.

Another important difference between this event and those from the convection tests is that the postevent frequency content is not concentrated at frequencies below 3 kHz. As seen in the spectro-

gram of trace C4 (Fig. 11), the energy in the response is focused at higher frequencies. Evidently, the response to the creak was felt only in high-frequency modes, localized in the vicinity of accelerometer C4. The three dominant modes of response are at 9, 14.5, and 18 kHz. Truncating and bandpass filtering the trace around the 9 kHz mode allowed the modal damping ratio to be estimated at around 2%, a reasonable level of damping for a local mode in a jointed structure predominantly made of Lexan. The damping estimates for the other two dominant modes yield values between 1 and 2%, as well.

Summary of Findings

In total, over 14 days of thermal testing, about 30 events were identified as thermal creaks. A detailed discussion of the results from the thermal tests can be found in Ref. 10. In general, certain common characteristics of thermal creak were identified, independent of the heat-transfer mechanism. First, the creaks were generally detected at propitious times: during thermal transients, after a significant change in temperature had occurred, but before steady state was attained throughout the structure. The disturbances themselves were impulsive and broadband in nature.

These characteristics of thermal creak disturbances were predicted in an analytical study.⁶ The transient response measurements exhibited telltale signs of structural behavior, including multimode or dominant-mode excitation, and reasonable amounts of modal damping in the decay of the response.

Beyond these common characteristics, however, several important differences were noted between creaks observed in the convection chamber and those observed in the thermal vacuum chamber. Overall, fewer thermal creaks were recorded during the radiation tests than during the convection tests. Furthermore, each event was only detected by one accelerometer on the truss during the radiation tests; the creak response was therefore far more localized than for the convection tests, where evidence of each event was generally detected across the entire truss. The highly localized nature of the disturbance was also reflected in the fact that creak response generally had content at significantly higher frequency in the radiation tests. These differences in the creak response are attributed to the different environments the truss was subjected to in the two types of test. The first, and perhaps most significant, difference in the test environments is the nature of the two heat-transfer

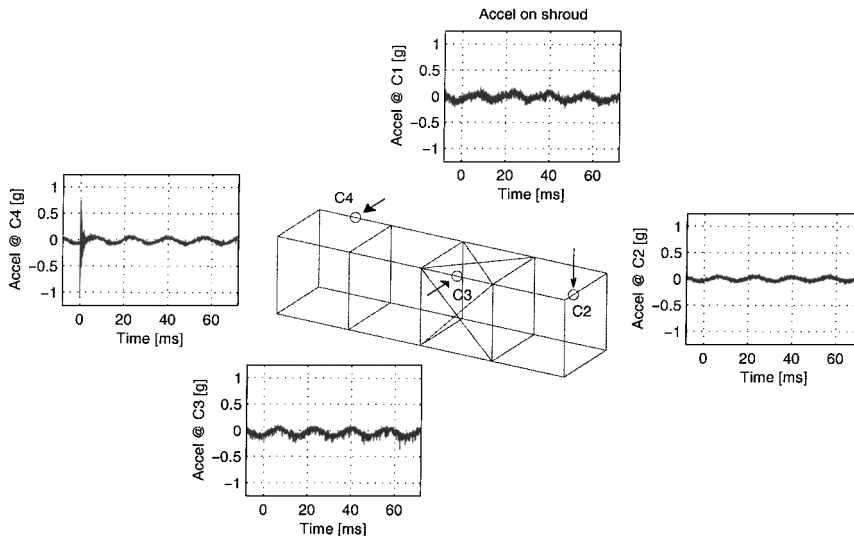


Fig. 10 Thermal creak data from a typical radiation test.

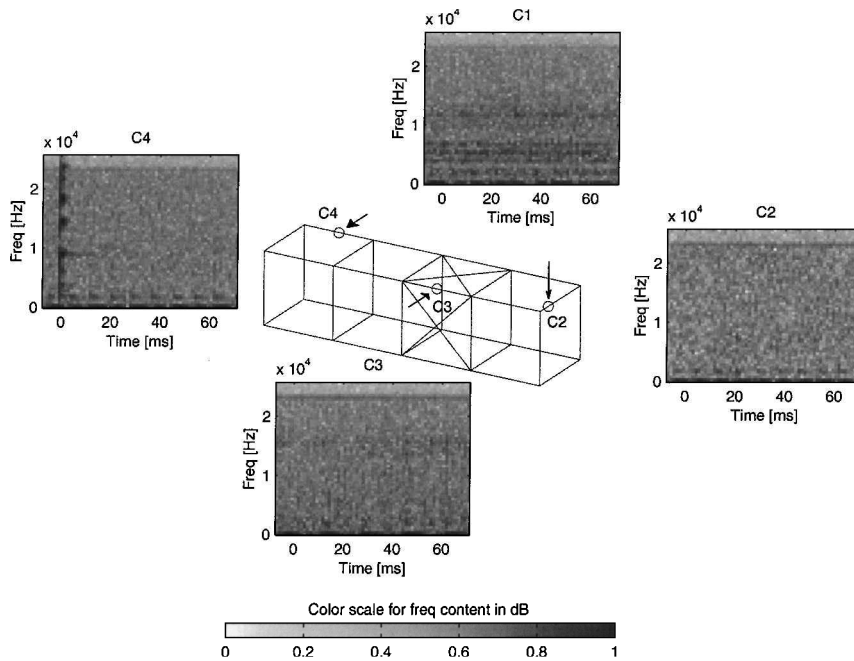


Fig. 11 Thermal creak event spectrograms from a typical radiation test.

processes. The blowing air in the convection chamber induced constant, low-frequency and relatively large-amplitude motion of the truss, whereas in the evacuated radiation chamber the test article remained comparatively still, feeling only the vibrations transmitted through the suspension system. It is reasonable to deduce that the constant dithering of the truss joints during the convection tests could have resulted in more frequent slips of the frictional interfaces and could also have affected the extent to which the disturbance is felt across the structure. Other important differences between the two types of test were the rate of temperature change and the temperature distribution across the truss. Further study would be required in order to gauge the effects of the faster cooling rate and nonuniform temperature distribution achieved in the radiation tests.

The frequency content of the truss response was found to vary significantly from event to event: the response to some creaks could only be seen at the lower end of the bandwidth of interest, below 3 kHz or so, whereas other creaks excited modes in the tens of kilohertz range. Generally, the peak acceleration amplitudes were found to be on the order of 0.1–1 g, although certain high-frequency events were observed which caused accelerations up to 20 g in magnitude. These acceleration levels correspond to displacement

vibration amplitudes estimated to be on the order of nanometers or greater.

Model Correlation

Because of the large number of potential creak elements in the truss, obtaining a deterministic creak model of the structure is impractical. Further, the creak source was not isolated in this experiment, and no data on the friction parameters or the joint behaviors exist. As a result, the actual location of the creak source, the creak frequency (inverse of creak period), and the magnitude of the dynamic response cannot be determined a priori. Information on the location of the sources, the magnitude of the response, and the propagation path can only be inferred from the data. Thus, a qualitative correlation between the experimental data and the model results is presented in this section.

Model Description

The creak source and location are qualitatively identified using the data from the typical convection test presented in the preceding section. For the event shown in Fig. 7, the dominant frequencies around 3 kHz are in the range of the predicted longeron axial modes.

Table 1 Numerical values of creak model parameters

Parameter	Value
κ	15
f_k	0.95
μ	0.073

As a result, the creak source is assumed to be the pin joint (shown in Fig. 4) slipping in the axial direction. Furthermore, the results indicated that the creak location was most likely to be between sensors C4 and C3. The location is therefore assumed to be one of the pin-clevis joints in the first bay.

Once the creak source and the slip mode are assumed, the truss structure is reduced to the simple model developed in Ref. 7 (Fig. 1). The first bay is represented by the creak element, and the attached single-degree-of-freedom system is now replaced with a multi-degree-of-freedom system representing the remainder of the structure. The slider shown in Fig. 1 represents the slipping longeron, and the pin represents the rest of the bay. The model parameters are extracted from an existing finite element model of the structure.¹² The stiffness matrix of a single bay without the slipping longeron was reduced via static condensation to k_1 , the stiffness associated with the degree of freedom at the friction interface. The axial stiffness of the strut k_2 is computed assuming a linear deflection. To approximate the effective modal mass m_1 , the frequency associated with the mode shape that most resembles the assumed slip deformation is used. The modal mass for the slipping longeron m_2 was approximated to match the first longitudinal mode frequency of the strut. No data on the friction parameters of the truss joints are available, and thus a relatively high value for the friction ratio f_k is assumed.

Using the parameters given in Table 1, a nonlinear creak analysis is performed on the model, resulting in a force history. The finite element model of the full truss was used to develop a state-space model of the system. Only modes in the 1.4–3 kHz range were included in the structural dynamics model. The force history is then applied to the state-space model at the node where the slip occurs. Further detail on the model and creak analysis is found in Ref. 7.

Model Results

The acceleration data were filtered to observe the response in the frequency range of interest (from 1.4 to 3 kHz). Because of the lack of data on the friction mechanism, another parameter in the model, the characteristic length, was approximated to match the amplitude of the vibrations obtained from the data. This characteristic length is the critical displacement at which a slip would occur under the condition that the thermal strain is zero.⁷ This parameter could be measured experimentally at the component level.

The correlation results are presented in Fig. 12. The results show that the model qualitatively captures the behavior. The shapes of the envelopes in the response match well. The relative magnitudes in the model results are in a good agreement with the data, considering only one parameter was fitted. The model, however, exhibits higher-frequency content. The frequencies do not match because of possible modeling errors in the finite element model. The discrepancies between the model and the data may also be caused by the assumptions about the location of the creak source. The attenuation of the signal away from the source is not apparent in the model results because the model does not capture the wave propagation characteristics. Finally, another possible source of error is the fact that a linear finite element model was used to model the nonlinear dynamics of the structure.

Sensitivity Analysis

To qualitatively investigate the effect of the parameters on the response, a preliminary sensitivity analysis was performed on the parameters f_k , κ , and μ , as well as the assumed creak location. Each parameter was varied from the nominal value, whereas the others retained the nominal values.

The magnitude of the response was found to be most sensitive to change in f_k . The resulting change in response magnitude was

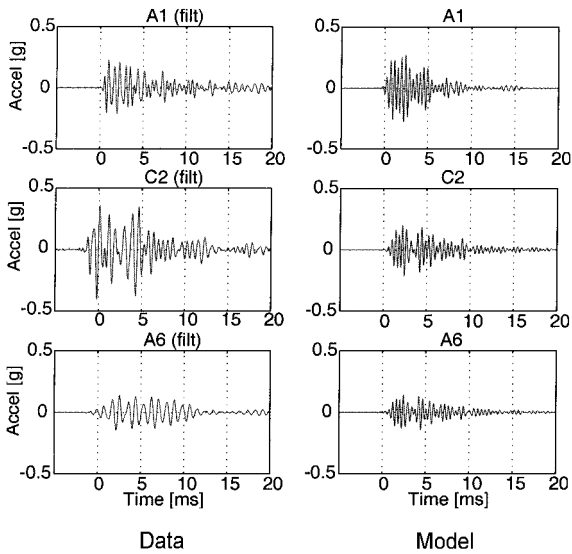


Fig. 12 Model correlation results.

linearly proportional to $(1 - f_k)$. The dynamic response of the creak element was a higher order effect, and as a result, any change in its mass ratio μ had a minimal effect on the magnitude of the system response. The envelope shapes of the responses were quite sensitive to κ and the creak location, whereas the magnitude of the response was relatively insensitive to the creak location. The relative magnitudes between sensors varied for different creak locations, as expected. Varying μ and κ affected the force history because the time between slip initiation and slip termination is a function of these parameters. As a result, different modes were excited, and a different mode mix resulted.

Conclusions

This thermal creak investigation confirmed that thermally induced transient events can indeed be observed on statically indeterminate structures with frictional interfaces. Furthermore, the thermal creak behavior can be captured in a relatively simple model of the nonlinear structural mechanism. During the suite of tests, the broadband response of a deployable truss structure to thermal creak disturbances was characterized. The creak events induced accelerations up to 20 g in magnitude on the structure, over frequencies ranging from hundreds of hertz up to tens of kilohertz; the corresponding displacements were estimated to be at least on the order of nanometers. These levels of transient response are of concern in the design of precision space structures: at such high frequencies (which lie beyond the bandwidth of the structural and optical control systems) vibrations of this amplitude could cause the precision optics to lose lock. This would foul up the measurement in progress and require valuable time to be spent on optical recapture.

The results from this investigation yield preliminary indications that certain actions can be taken to mitigate the thermal creak problem. If creaks primarily excite local dynamics, as observed in the tests performed in the thermal vacuum chamber, it may be possible to design the structure such that its sensitive instruments are isolated from the propagation path of the transient disturbance. As an alternative to designing around the creak problem, it may be preferable to make efforts to avoid it altogether. One way would be to design the structure such that differential thermal expansion is minimized (by balancing the CTEs across the structure and making the thermal environment as uniform as possible or by using a statically determinate structure). Also, it may be possible to eliminate from the spacecraft design many of the potential nonlinear energy release mechanisms.

Acknowledgments

This research was sponsored by the Jet Propulsion Laboratory (JPL) at the California Institute of Technology. The authors greatly appreciate the support of the project technical monitor at JPL, Marie Levine. The authors would also like to thank the following people

for their patience and generosity in allowing use of their facilities for the thermal creak experiment: Marthinus van Schoor of Mide Technology Corp., Javier de Luis of Payload Systems, Inc., and Ed Mencow, Ron Efromson, Jon Howell, and Al Mason from Massachusetts Institute of Technology Lincoln Laboratory.

References

- ¹Allen, R. J., Peterson, D., and Shao, M., "Space Interferometry Mission—Taking Measure of the Universe," *Optical Telescopes of Today and Tomorrow: Proceedings of the International Society for Optical Engineering*, Vol. 2871, edited by A. L. Ardeberg, Society of Photo-Optical Instrumentation Engineers, Bellingham, WA, 1997, pp. 504–515.
- ²Zimbelman, D. F., and Zimbelman, H. F., "Self-Induced Thermal Elastic Shock Disturbance for a Dual-Array Spinning Spacecraft," *American Astronautical Society*, Paper 91-147, Feb. 1991.
- ³Foster, R. S., and Thornton, E. A., "An Experimental Investigation of Thermally Induced Vibrations of Spacecraft Structures," *Proceedings of the 35th AIAA Structures, Structural Dynamics, and Materials Conference*, AIAA, Washington, DC, 1994, pp. 584–596.
- ⁴Thornton, E. A., *Thermal Structures for Aerospace Applications*, AIAA Education Series, AIAA, Reston, VA, 1996, pp. 343–396.
- ⁵Foster, C. L., Tinker, M. L., Nurre, G. S., and Till, W. A., "The Solar Array-Induced Disturbance of the Hubble Space Telescope Pointing System," *Journal of Spacecraft and Rockets*, Vol. 32, No. 4, 1995, pp. 634–644.
- ⁶Kim, Y. A., and McManus, H. L., "Thermally-Induced Vibrations of Space Structures," *Thermal Stresses '97: Proceedings of the Second International Symposium on Thermal Stresses and Related Topics*, Rochester, NY, 1997, pp. 661–664.
- ⁷Kim, Y. A., McManus, H. L., and Miller, D. W., "Thermal Creak Induced Dynamics of Space Structures," Space Engineering Research Center, Massachusetts Inst. of Technology, SERC Rept. 14-98, Cambridge, MA, Nov. 1998.
- ⁸Levine, M. B., "The Interferometry Program Flight Experiments: IPEX I and II," *Astronomical Interferometry: Proceedings of the International Society for Optical Engineering*, Vol. 3350, edited by R. D. Reasenberg, Society of Photo-Optical Instrumentation Engineers, Bellingham, WA, 1998, pp. 707–718.
- ⁹Crawley, E. F., Barlow, M. S., van Schoor, M. C., Masters, B., and Bixos, A. S., "Measurement of the Modal Parameters of a Space Structure in Zero Gravity," *Journal of Guidance, Control, and Dynamics*, Vol. 18, No. 3, 1995, pp. 385–394.
- ¹⁰Ingham, M. D., Crawley, E. F., and Miller D. W., "Microdynamics and Thermal Snap Response of Deployable Space Structures," Space Engineering Research Center, Massachusetts Inst. of Technology, SERC Rept. 2-98, Cambridge, MA, May 1998.
- ¹¹Doyle, J. F., *Wave Propagation in Structures: An FFT-Based Spectral Analysis Methodology*, 1st ed., Springer-Verlag, New York, 1989, p. 69.
- ¹²Barlow, M. S., and Crawley, E. F., "The Dynamics of Deployable Truss Structures in Zero-Gravity: The MODE STA Results," Space Engineering Research Center, Massachusetts Inst. of Technology, SERC Rept. 1-92, Cambridge, MA, Jan. 1992.

R. B. Malla
Associate Editor